 CMES, vol.115, no.1, pp.1-24, 2018

Statistical Multiscale Analysis of Transient Conduction and Radiation Heat Transfer Problem in Random Inhomogeneous Porous Materials

Yiqiang Li[1], Liang Ma[2], Zhiqiang Yang[3], Xiaofei Guan[4], Yufeng Nie[1] and Zihao Yang[1, 2, *]

Abstract: This paper is devoted to the homogenization and statistical multiscale analysis of a transient heat conduction problem in random porous materials with a nonlinear radiation boundary condition. A novel statistical multiscale analysis method based on the two-scale asymptotic expansion is proposed. In the statistical multiscale formulations, a unified linear homogenization procedure is established and the second-order correctors are introduced for modeling the nonlinear radiative heat transfer in random perforations, which are our main contributions. Besides, a numerical algorithm based on the statistical multiscale method is given in details. Numerical results prove the accuracy and efficiency of our method for multiscale simulation of transient nonlinear conduction and radiation heat transfer problem in random porous materials.

Keywords: Statistical multiscale analysis method, transient heat conduction problem, nonlinear radiation boundary condition, random porous materials.

1 Introduction

With rapid developments of space aircraft in recent years, porous materials have been widely used as insulation for thermal protection system owing to their various elegant qualities, such as low relative density, high heat resistance, low thermal conductivity and high radiation attenuation coefficient compared to the traditional materials [Grujicic, Pandurangan, Zhao et al. (2006); Ishizaki, Komarneni and Nanko (2013)]. And it is important to understand the thermal responses of porous materials and structures in many engineering applications. As we know, heat transfer in porous materials contains conduction, convection and radiation. The convective heat transfer can be neglected in closed-cell porous materials and radiation is typically the major mode of heat transfer in high-porosity insulations at high temperature environment [Modest (2013)].

Porous materials usually have multiple length scales [Park and Hou (2004); Zhang, Yang, Zhang et al. (2013); Wu and Xiao (2017)] and random microscopic configurations [Sundén

[1] Department of Applied Mathematics, Northwestern Polytechnical University, Xi'an 710072, China.

[2] State Key Laboratory of Solidification Processing, Northwestern Polytechnical University, Xi'an 710072, China.

[3] School of Astronautics, Harbin Institute of Technology, Harbin 150001, China.

[4] School of Mathematics Sciences, Tongji University, Shanghai 200092, China.

[*] Corresponding author: Zihao Yang. Email: yangzihao@nwpu.edu.cn.

and Yuan (2013); Wang, Wang, Pan et al. (2007)]. According to the arrangement characteristics of perforations, random materials can be classified into materials with consistent random distribution and those with inconsistent random distribution [Li and Cui (2005); Han, Cui and Yu (2010)]. The consistent random distribution means that the volume fraction and probability distribution model of perforations are the same everywhere in porous materials (Fig. 1), which will be considered in this paper. Considering interior surface radiation effect in the closed-cells, heat transfer response of random porous materials would become much complicated. Therefore, it is necessary to study the heat conduction-radiation problem of random porous materials.

Up to now, some theoretical models have been proposed and employed to calculate the effective thermal conductivity properties of composite materials, such as Maxwell-Eucken model [Hashin and Shtrikman (1962)], generalized self-consistent method [Chou, Nomura and Taya (1980)], Cheng-Vachon model [Cheng and Vachon (1969)], self-consistent method [Hill (1965)]. However, these methods simplified the microstructure of real composite materials by the homogenization schemes in order to reduce the computational complexity. Moreover, by using these theoretical methods the local temperature fields cannot be calculated. Some works have been performed on heat conduction-radiation problem of porous materials. Liu et al. [Liu and Zhang (2006)] calculated the effective macroscopic properties of static heat conduction-radiation problem. Allaire et al. [Allaire and El Ganaoui (2009)] gave the homogenization process of heat conduction problem with non-classical radiation boundary conditions by two-scale asymptotic expansion. It should be pointed out that the non-classical model cannot be used for the porous materials with low porosity, because it over-estimates the radiation behavior on the interior surface of cavities. The homogenization solutions of the heat conduction problem with radiation boundary condition were obtained in Bakhvalov [Bakhvalov (1981)]. After that, Yang et al. [Yang, Cui, Nie et al. (2012)] presented a second-order two-scale analysis method for the heat transfer problem of periodic porous materials with interior surface radiation. Besides, Amosov [Amosov (2010)] and Tiihonen [Tiihonen (1997)] proved the existence and uniqueness of the heat conduction equation with nonlinear radiation boundary conditions.

To our knowledge, we have not seen the study of the transient heat transfer problem of random porous materials with interior surface radiation in the existing literature. Actually, random porous materials have been widely used in engineering, such as metal-matrix composites and polymer blends. The transient heat conduction-radiation model is nonlinear, and it is difficult to find the analytical solutions. As for numerical solutions, due to the random structures and characteristic coefficients oscillating rapidly in small cells, in order to effectively capture the local fluctuation behaviors of temperature field and its derivatives, the mesh size must be very small while employing the traditional numerical methods, which will lead to tremendous amount of computer memory and CPU time. Therefore, it is necessary to develop highly efficient numerical method to solve the nonlinear transient heat conduction-radiation problem of random porous materials.

The homogenization method is developed to describe the overall behaviors of composite materials by incorporating the fluctuations due to the heterogeneities of the composites materials [Bensoussan, Lions and Papanicolaou (2011)]. However, numerous numerical

results have demonstrated that the numerical accuracy of the standard homogenization method may not be satisfactory [Efendiev and Hou (2009); Yang, Zhang, Dong et al. (2017)]. And then, based on the homogenization method, various multi-scale methods have been proposed [Efendiev and Hou (2009); Juanes (2005); Engquist, Li, Ren et al. (2007)]. However, they only obtained first-order asymptotic expansions, which are not enough to capture the local fluctuations of solutions in many physical and mechanical problems. Hence, it is necessary to develop more effective methods, which is the motivation for seeking higher-order multiscale methods. The existences of homogenization coefficients and homogenization solutions for the composite materials with consistent random distribution were proved in Jikov et al. [Jikov, Kozlov and Oleinik (2012)]. Cui et al. [Cui, Shih and Wang (1999); Yang, Ma and Ma (2017)] introduced the second-order multiscale method to predict different physical and mechanical behaviors of composite structures. By adding the second-order correctors, the microscopic fluctuation behaviors inside the composite materials can be captured more accurately. For the random composite material, Cui et al. [Li and Cui (2005); Guan, Liu, Jia et al. (2015); Han, Cui and Yu (2010)] established a statistical multiscale method by introducing a random sample cell. However, previous multiscale method cannot be directly applied to the transient conduction and radiation heat transfer problem because of the nonlinearity, randomness and time variation. Up to now, there is no effective numerical method found for the transient and nonlinear heat transfer problem of random porous materials.

The aim of this paper is to develop a novel statistical multiscale analysis method for the transient heat conduction problem in random porous materials with a nonlinear radiation boundary condition. The remainder of this paper is outlined as follows. In Section 2, the microscopic representation of random porous materials and the transient heat conduction-radiation model are given. The formulation of multiscale asymptotic expansion is derived and the finite element algorithms based on the statistical multiscale method are given in details in Section 3. In Section 4, numerical results obtained by the statistical multiscale method are given to demonstrate the effectiveness of the present method. Finally, some conclusions are presented in Section 5. For convenience, we use the Einstein summation convention on repeated indices in this paper.

2 Transient conduction and radiation heat transfer problem

In this section, the microscopic representation of random porous materials is described. And then the transient heat conduction equation with a nonlinear radiation boundary condition is presented.

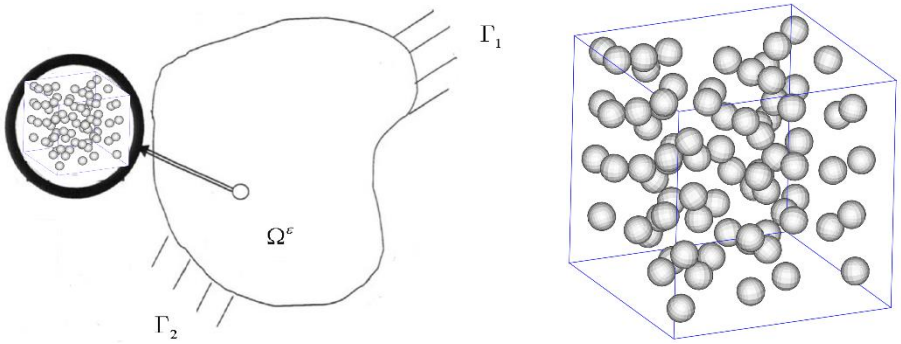

(a) (b)

Figure 1: Porous materials with random distribution of pores (a) The whole structure Ω^ε ; (b) Unit cell Y^{*s}

2.1 Microscopic representation of random porous materials

Suppose that the investigated porous material structure Ω^ε is made from matrix and pores. All the pores are considered as ellipsoids, which are randomly distributed in the matrix. In this paper, all the ellipsoid pores are considered as "one-scale", which means all of their long axes satisfy $r_1 < a < r_2$ where r_1 and r_2 are given lower and upper bounds. And porous materials with random distribution of pores can be represented as follows

1) There exists a constant ε satisfying $r_2 \ll \varepsilon \ll L$, where L denotes the size of Ω^ε. Thus Ω^ε can be considered as a set of cells with size ε, as shown in Fig. 1(a).
2) Each ellipsoid in three-dimensional apace is defined by 9 random parameters, i.e. the coordinates of the central point (x_{01}, x_{02}, x_{03}), the sizes of the long, middle and short axis (a_1, a_2, a_3) and 3 orientation parameters of the long and middle axis $(\beta_1, \beta_2, \beta_3)$. Let $\xi = (a_1, a_2, a_3, \beta_1, \beta_2, \beta_3, x_{01}, x_{02}, x_{03})$, which contains all the information of an ellipsoid. If there are K ellipsoids in a cell εY^s, Y^s represents a normalized cell, then a random sample ω^s can be defined as $\omega^s = (\xi_1^s, \xi_2^s, \xi_3^s, \cdots, \xi_{K-1}^s, \xi_K^s)$.

The distribution of the pores in each cell satisfies the same probability distribution function. Then the investigated structure has periodically random distribution of pores, and then can be represented by the probability distribution of pores inside a typical cell. Therefore, the porous structure Ω^ε is logically composed of ε- size cells subjected to the identical probability distribution model P and

$$\Omega^\varepsilon = \bigcup_{s=1}^{m}{}_{(\omega^s, z\in Z)} \varepsilon(Y^s + z)$$

where $s = 1,2,3...,m$ denotes the index of samples and Z is the integer set. For the whole Ω^ε, define

$$\omega = \left\{ \omega^s \,\middle|\, x \in \varepsilon Y^s \subset \Omega^\varepsilon \right\}$$

Thus the thermal conductivity parameters of random porous materials can be considered by

$$\left\{k_{ij}^{\varepsilon}(x,\omega^s)\right\} = k_{ij}^1, \quad \text{if} \quad x \in \varepsilon Y^s - \bigcup_{k=1}^{K} e_k$$

where e_k denotes the kth pore inside εY^s, and the material coefficient k_{ij}^1 satisfies that $\left|k_{ij}^1\right| < C$, where C is a positive constant.

2.2 Heat conduction-radiation equation

Let $Y = \left\{y : 0 \le y_j \le 1,\ j = 1,2,3\right\}$ and ϖ be a smooth unbounded domain in R^3 with random structures satisfying following conditions [Oleinik, Shamaev and Yosifian (1992)]:

1) The unit cell $Y^* = \varpi \bigcap Y$ is a domain with a Lipschitz boundary. $\partial Y^* = \partial Y \bigcup \Gamma$ and Γ is the surfaces of cavities and Y^* is the solid part of Y, shown in Fig. 1(b).
2) The set $Y \setminus \bar{\varpi}$ ($\bar{\varpi}$ stands for the closure in R^3 of the domain ϖ) and the intersection of $Y \setminus \bar{\varpi}$ with δ_0 neighborhood of ∂Y consist of a finite number of Lipschitz domains separated from each other and from the edges of Y by a positive distance.

The cavities of the domain are convex. Then, the investigated porous domain Ω^{ε} as shown in Fig. 1(a) can be expressed as $\Omega^{\varepsilon} = \Omega \bigcap \varepsilon\varpi$, where Ω is a bounded convex domain in R^3 without cavities, and these cavities do not intersect with $\partial\Omega$.

Suppose that the radiative surfaces of cavities are diffuse and grey, that is, the emissivity e of the surfaces does not depend on the wavelength of radiation. And based on the modeling of heat radiative process by an integral equation on the surfaces of cavities in periodic structures [Liu and Zhang (2006)] and microscopic representation of random structures, the nonlinear radiation boundary condition on interior surfaces of closed cavities in random porous materials can be defined as

$$-\nu_i k_{ij}^{\varepsilon}(x,\omega)\frac{\partial T_{\varepsilon}(x,\omega,t)}{\partial x_j} = e\sigma T_{\varepsilon}^4(x,\omega,t) - e\int_{\Gamma_{\varepsilon,m}^c} R_{\varepsilon}(x,\omega,t)F(x,z)dz$$

where $T_{\varepsilon}(x,\omega,t)$ denotes the temperature, σ the Stefan-Boltzmann constant, $\mathbf{\nu} = (\nu_i)$ the unit outward normal on Γ_{ε}^c; $\Gamma_{\varepsilon}^c = \bigcup_{m=1}^{m(\varepsilon)} \Gamma_{\varepsilon,m}^c$ is the boundary composed of interior surfaces of cavities $\Gamma_{\varepsilon,m}^c$, and $m(\varepsilon)$ the number of cavities in porous materials; the emissivity e satisfies $0 < e \le 1$ and $R_{\varepsilon}(x,\omega)$ is the intensity of emitted radiation given by

$$R_{\varepsilon}(x,\omega,t) = e\sigma T_{\varepsilon}^4(x,\omega,t) + (1-e)\int_{\Gamma_{\varepsilon,m}^c} R_{\varepsilon}(z,\omega,t)F(x,z)dz, \quad \forall x \in \Gamma_{\varepsilon,m}^c$$

where $F(x,z)$ is the view factor between two different points x and z on $\Gamma_{\varepsilon,m}^c$, and is defined on three dimensional form for a convex cavity as follows [Allaire and El Ganaoui (2009)]

$$F(x,z) = \frac{n_z(x-z)n_x(z-x)}{\pi\left|z-x\right|^4}$$

where n_z and n_x denote the unit normal at different points z and x on $\Gamma^c_{\varepsilon,m}$, respectively. And for any $(x,z)\in(\Gamma^c_{\varepsilon,m})^2$, it satisfies the following properties

$$F(x,z)\geq 0,\ F(x,z)=F(z,x),\ \int_{\Gamma^c_{\varepsilon,m}} F(x,z)dz=1$$

Under aforementioned assumptions, the transient heat transfer problem in random porous structures can be expressed as follows

$$\rho^{\varepsilon}(x,\omega)c^{\varepsilon}(x,\omega)\frac{\partial T_{\varepsilon}(x,\omega,t)}{\partial t}-\frac{\partial}{\partial x_i}\left(k^{\varepsilon}_{ij}(x,\omega)\frac{\partial T_{\varepsilon}(x,\omega,t)}{\partial x_j}\right)=f(x,t) \tag{1}$$

The corresponding initial and thermal boundary conditions are

$$T_{\varepsilon}(x,\omega,t)=\bar{T}(x,t),\quad (x,t)\in\Gamma_1\times(0,t_*)$$

$$\nu_i k^{\varepsilon}_{ij}(x,\omega)\frac{\partial T_{\varepsilon}(x,\omega,t)}{\partial x_j}=0,\quad (x,t)\in\Gamma_2\times(0,t_*)$$

$$T_{\varepsilon}(x,\omega,0)=T_{in}(x),\quad x\in\Omega^{\varepsilon}$$

$$-\nu_i k^{\varepsilon}_{ij}(x,\omega)\frac{\partial T_{\varepsilon}(x,\omega,t)}{\partial x_j}$$

$$=e\sigma T^4_{\varepsilon}(x,\omega,t)-e\int_{\Gamma^c_{\varepsilon,m}} R_{\varepsilon}(x,\omega,t)F(x,z)dz,\quad (x,t)\in\Gamma^c_{\varepsilon}\times(0,t_*)$$

where $i,j=1,2,3$; $\rho^{\varepsilon}(x,\omega)$, $c^{\varepsilon}(x,\omega)$ and $k^{\varepsilon}_{ij}(x,\omega)$ are the mass density, specific heat and thermal conductivity, respectively; $f(x,t)$ denotes the internal heat source, $\bar{T}(x,t)$ the prescribed boundary temperature, Γ_1 and Γ_2 the parts of the boundary of this region, where temperature and heat flux are specified such that $\Gamma_1\bigcup\Gamma_2=\partial\Omega,\Gamma_1\cap\Gamma_2=\varnothing$. The time $t\in(0,t_*)$ plays the role of a parameter and t_* denotes the upper bound of time.

In order to avoid the arguments on the mathematical properties of investigated functions below, we suppose that the random material parameters $\left\{k^{\varepsilon}_{ij}(x,\omega^s)\right\}$ are bounded measurable functions of the random variable ω^s, and their mathematical expectations exist. Besides, $\left\{k^{\varepsilon}_{ij}(x,\omega^s)\right\}$ is supposed to be symmetric.

3 Statistical multiscale method

In this section, the statistical multiscale formulation is derived by using the constructive way for calculating the nonlinear transient heat conduction behaviors of random porous materials. Moreover, the corresponding numerical algorithm is presented in details.

3.1 Statistical multiscale asymptotic expansions

Introducing the variable $y=x/\varepsilon\in Y^s$ for ω^s, which denotes the local coordinates defined on 1-normalized cell Y^s, and then the material coefficients of microstructure in Y^s can be

expressed as $\rho^{\varepsilon}(x,\omega)=\rho(y,\omega^s)$, $c^{\varepsilon}(x,\omega)=c(y,\omega^s)$ and $k_{ij}^{\varepsilon}(x,\omega)=k_{ij}(y,\omega^s)$. Since the temperature solution $T_{\varepsilon}(x,\omega,t)$ of the heat conduction problem (1) depends on both global behaviors of the structure Ω^{ε} and local configuration in Y^s, and then it can be expressed as $T_{\varepsilon}(x,\omega,t)=T(x,y,\omega^s,t)$. In this paper, it is supposed that $e=1$ to simplify the exposition. However, it is easy to extend the case $0<e<1$, see Park et al. [Park and Hou (2004)] for details. Further, it is assumed that $T_{\varepsilon}(x,\omega,t)$ can be expanded into the following form in two-scale variables x and y

$$\begin{aligned}T_{\varepsilon}(x,\omega,t)&=T_0(x,t)+\varepsilon N_{\alpha_1}(y,\omega^s)\frac{\partial T_0(x,t)}{\partial x_{\alpha_1}}+\varepsilon^2\left(N_{\alpha_1\alpha_2}(y,\omega^s)\frac{\partial^2 T_0(x,t)}{\partial x_{\alpha_1}\partial x_{\alpha_2}}\right.\\&\left.+C_{\alpha_1}(y,\omega^s)T_0^3(x,t)\frac{\partial T_0(x,t)}{\partial x_{\alpha_1}}+M(y,\omega^s)\frac{\partial T_0(x,t)}{\partial t}\right)+\varepsilon^3 P_1(x,y,\omega^s,t),\quad x\in\Omega^{\varepsilon},\ y\in Y^{*s}\end{aligned}\tag{2}$$

where $T_0(x,t)$ is the homogenization solution, which only reflects macroscopic behaviors, $N_{\alpha_1}(y,\omega^s)$, $N_{\alpha_1\alpha_2}(y,\omega^s)$, $C_{\alpha_1}(y,\omega^s)$ and $M(y,\omega^s)$ are called as local solutions. Due to $y=x/\varepsilon\in Y^s$, Differentiation with respect to x is defined as

$$\frac{\partial}{\partial x_i}\to\frac{\partial}{\partial x_i}+\frac{1}{\varepsilon}\frac{\partial}{\partial y_i}\tag{3}$$

We now substitute (2) into (1) and match terms of the same order of ε, then the following equations can be obtained

$$\begin{aligned}&\rho^{\varepsilon}(x,\omega^s)c^{\varepsilon}(x,\omega^s)\frac{\partial T_{\varepsilon}(x,\omega^s,t)}{\partial t}-\frac{\partial}{\partial x_i}\left(k_{ij}^{\varepsilon}(x,\omega^s)\frac{\partial T_{\varepsilon}(x,\omega^s,t)}{\partial x_j}\right)\\&=-\varepsilon^{-1}\frac{\partial}{\partial y_i}\left(k_{ij}(y,\omega^s)\left(\frac{\partial T_0(x,t)}{\partial x_j}+\frac{\partial N_{\alpha_1}(y,\omega^s)}{\partial y_j}\frac{\partial T_0(x,t)}{\partial x_{\alpha_1}}\right)\right)\\&-\varepsilon^0\left(k_{ij}(y,\omega^s)\frac{\partial^2 T_0(x,t)}{\partial x_i\partial x_j}+k_{ij}(y,\omega^s)\frac{\partial N_{\alpha_1}(y,\omega^s)}{\partial y_j}\frac{\partial^2 T_0(x,t)}{\partial x_i\partial x_{\alpha_1}}\right.\\&+\frac{\partial}{\partial y_i}\left(k_{ij}(y,\omega^s)N_{\alpha_1}(y,\omega^s)\right)\frac{\partial^2 T_0(x,t)}{\partial x_j\partial x_{\alpha_1}}+\frac{\partial}{\partial y_i}\left(k_{ij}(y,\omega^s)\frac{\partial N_{\alpha_1\alpha_2}(y,\omega^s)}{\partial y_j}\right)\frac{\partial^2 T_0(x,t)}{\partial x_{\alpha_1}\partial x_{\alpha_2}}\\&+\frac{\partial}{\partial y_i}\left(k_{ij}(y,\omega^s)\frac{\partial C_{\alpha_1}(y,\omega^s)}{\partial y_j}\right)T_0^3(x,t)\frac{\partial T_0(x,t)}{\partial x_{\alpha_1}}\\&\left.+\frac{\partial}{\partial y_i}\left(k_{ij}(y,\omega^s)\frac{\partial M(y,\omega^s)}{\partial y_j}\right)\frac{\partial T_0(x,t)}{\partial t}-\rho(y,\omega^s)c(y,\omega^s)\frac{\partial T_0}{\partial t}\right)+O(\varepsilon)=f(x,t),\end{aligned}\tag{4}$$

$$
\begin{aligned}
&-\nu_i k_{ij}^{\varepsilon}(x,\omega^s)\frac{\partial T_{\varepsilon}(x,\omega^s,t)}{\partial x_j} \\
&=\sigma T_{\varepsilon}^4(x,\omega^s,t)-\sigma\int_{\Gamma_{\varepsilon,m}^c} T_{\varepsilon}^4(x,\omega^s,t)F(x,z)dz=\sigma T_0^4(x,t)-\sigma\int_{\Gamma^c} T_0^4(x,t)F(y,s)ds \\
&+\varepsilon 4\sigma T_0^3(x,t)\frac{\partial T_0(x,t)}{\partial x_{\alpha_1}}\left(N_{\alpha_1}(y,\omega^s)-\int_{\Gamma^c} N_{\alpha_1}(s,\omega^s)F(y,s)ds\right)+O(\varepsilon^2).
\end{aligned} \tag{5}
$$

A series of equations are obtained if the coefficients of $\varepsilon^l (l=-1,0,1,2,\cdots)$ from both sides of above equations are required to equal to each other.

From the coefficients of ε^{-1} the following local problem defined on Y^{*s} for $N_{\alpha_1}(y,\omega^s)$ are constructed

$$
\begin{cases}
\dfrac{\partial}{\partial y_i}\left(k_{i\alpha_1}(y,\omega^s)+k_{ij}(y,\omega)\dfrac{\partial N_{\alpha_1}(y,\omega^s)}{\partial y_j}\right)\dfrac{\partial T_0(x,t)}{\partial x_{\alpha_1}}=0, \quad \text{in } Y^{*s} \\
-\nu_i\left(k_{ij}(y,\omega^s)\dfrac{\partial N_{\alpha_1}(y,\omega^s)}{\partial y_j}+k_{i\alpha_1}(y,\omega^s)\right)\dfrac{\partial T_0(x,t)}{\partial x_{\alpha_1}} \\
=\sigma T_0^4(x,t)-\sigma\int_{\Gamma^c} T_0^4(x,t)F(y,s)ds, \qquad y\in\Gamma
\end{cases} \tag{6}
$$

where Γ is the interior surfaces of the cavities contained in Y^{*s}, as shown in Fig. 2(b), such that $\Gamma=\bigcup_{n=1}^{N}\Gamma_n^c$, and N the number of cavities contained in the unit cell Y^{*s}. Considering

$$\int_{\Gamma^c} F(y,s)ds=1,$$

it is easy to get that

$$\sigma T_0^4(x,t)-\sigma\int_{\Gamma^c} T_0^4(x,t)F(y,s)ds=0 \tag{7}$$

Since $\partial T_0(x,t)/\partial x_{\alpha_1}$ arises from the macroscopic behavior of the structure, it is not identical to zero. By virtue of (7), (6) can be rewritten as

$$
\begin{cases}
\dfrac{\partial}{\partial y_i}\left(k_{ij}(y,\omega^s)\dfrac{\partial N_{\alpha_1}(y,\omega^s)}{\partial y_j}\right)=-\dfrac{\partial k_{i\alpha_1}(y,\omega^s)}{\partial y_i}, \text{ in } Y^{*s} \\
-\nu_i\left(k_{ij}(y,\omega^s)\dfrac{\partial N_{\alpha_1}(y,\omega^s)}{\partial y_j}+k_{i\alpha_1}(y,\omega^s)\right)=0, \ y\in\Gamma
\end{cases} \tag{8}
$$

To attach the following boundary condition on ∂Y^s

$$N_{\alpha_1}(y,\omega^s)=0 \quad \text{on} \quad \partial Y^s \tag{9}$$

Therefore, for any sample ω^s, $N_{\alpha_1}(y,\omega^s)$ is the solution of the following problem

$$\begin{cases} \dfrac{\partial}{\partial y_i}\left(k_{ij}(y,\omega^s \dfrac{\partial N_{\alpha_1}(y,\omega^s)}{\partial y_j} \right) = -\dfrac{\partial k_{i\alpha_1}(y,\omega^s)}{\partial y_i}, \quad \text{in } Y^{*s} \\ -\nu_i \left(k_{ij}(y,\omega^s)\dfrac{\partial N_{\alpha_1}(y,\omega^s)}{\partial y_j} + k_{i\alpha_1}(y,\omega^s) \right) = 0, \quad y \in \Gamma \\ N_{\alpha_1}(y,\omega^s) = 0, \qquad\qquad y \in \partial Y^s \end{cases} \tag{10}$$

Inspired by Li et al. [Li and Cui (2005)] and from $N_{\alpha_1}(y,\omega^s)$, for any fixed sample ω^s, the homogenization coefficients can be defined as

$$\begin{aligned} \hat{k}_{ij}(\omega^s) &= \frac{1}{\left|Y^{*s}\right|}\int_{Y^{*s}} \left(k_{ip}(y,\omega^s)\frac{\partial N_j(y,\omega^s)}{\partial y_p} + k_{ij}(y,\omega^s) \right) dy \\ \hat{S}(\omega^s) &= \frac{1}{\left|Y^{*s}\right|}\int_{Y^{*s}} \rho(y,\omega^s) c(y,\omega^s) dy \end{aligned} \tag{11}$$

where $\left|Y^{*s}\right|$ denotes the Lebesgue measure of Y^{*s}. From the symmetry and boundness of $\rho(y,\omega^s)$, $c(y,\omega^s)$, $k_{ij}(y,\omega^s)$ and Lemma 3.2 in [Li and Cui (2005)], it follows that $\hat{S}(\omega^s)$ and $\hat{k}_{ij}(\omega^s)$ are bounded functions of random variable and their mathematical expectations exist. Thus, by taking L samples $\omega^s (\mathrm{s} = 1,2,\cdots,L)$, L homogenization coefficients are obtained, and then according to the Kolmogorov's classical strong law of large number, one can calculate the expected homogenization coefficients in formulas

$$\bar{k}_{ij} = \lim_{L\to\infty} \frac{\sum_{s=1}^{L} \hat{k}_{ij}(\omega^s)}{L}, \bar{S} = \lim_{L\to\infty} \frac{\sum_{s=1}^{L} \hat{S}(\omega^s)}{L} \tag{12}$$

Further, one can define the homogenized problem associated with (1) as follows

$$\begin{cases} \bar{S}\dfrac{\partial T_0(x,t)}{\partial t} - \dfrac{\partial}{\partial x_i}\left(\bar{k}_{ij}\dfrac{\partial T_0(x,t)}{\partial x_j} \right) = f(x,t) \\ \qquad\qquad (x,t) \in \Omega \times (0,t_*) \\ T_0(x,t) = \bar{T}(x,t), \qquad (x,t) \in \Gamma_1 \times (0,t_*) \\ \nu_i \hat{k}_{ij}\dfrac{\partial T_0(x,t)}{\partial x_j} = 0, \qquad (x,t) \in \Gamma_2 \times (0,t_*) \\ T_0(x,0) = T_{in}(x), \qquad x \in \Omega \end{cases} \tag{13}$$

Similarly to Li et al. [Li and Cui (2005)], it is easy to prove that $\bar{k}_{ij}$ is symmetric, positive and definite. By Lax-Milgram theorem and Poincare's inequality, the homogenized problem (13) has a unique solution.

Next, comparing the coefficient of ε^0 on both sides of (4) and taking into account the homogenized Eq. (13), it can be obtained that

$$
\begin{aligned}
&\left(\bar{k}_{\alpha_1\alpha_2}(x)-\frac{\partial}{\partial y_i}\left(k_{i\alpha_2}(y,\omega^s)N_{\alpha_1}(y,\omega^s)\right)-k_{\alpha_1\alpha_2}(y,\omega^s)\right.\\
&-k_{\alpha_2 j}(y,\omega^s)\frac{\partial N_{\alpha_1}(y,\omega^s)}{\partial y_j}-\frac{\partial}{\partial y_i}\left(k_{ij}(y,\omega^s)\frac{\partial N_{\alpha_1\alpha_2}(x,y,\omega^s)}{\partial y_j}\right)\Bigg)\frac{\partial^2 T_0(x,t)}{\partial x_{\alpha_1}\partial x_{\alpha_2}}\\
&+\left(-\frac{\partial}{\partial y_i}\left(k_{ij}(y,\omega^s)\frac{\partial H_{\alpha_1}(x,y,\omega^s)}{\partial y_j}\right)+\frac{\partial\bar{k}_{\alpha_1\alpha_2}(x)}{\partial x_{\alpha_2}}\right)\frac{\partial T_0(x,t)}{\partial x_{\alpha_1}}\\
&+\frac{\partial}{\partial y_i}\left(k_{ij}(y,\omega^s)\frac{\partial C_{\alpha_1}(y,\omega^s)}{\partial y_j}\right)T_0^3(x,t)\frac{\partial T_0(x,t)}{\partial x_{\alpha_1}}\\
&+\left(-\frac{\partial}{\partial y_i}\left(k_{ij}(y,\omega^s)\frac{\partial M(y,\omega^s)}{\partial y_j}\right)+\rho(y,\omega^s)c(y,\omega^s)-\bar{S}(x)\right)\frac{\partial T_0(x,t)}{\partial t}=0
\end{aligned}
\tag{14}
$$

Since $\partial^2 T_0(x,t)/\partial x_{\alpha_1}\partial x_{\alpha_2}$, $\partial T_0(x,t)/\partial x_{\alpha_1}$ and $\partial T_0(x,t)/\partial t$ are not identical to zero and considering the radiation asymptotic expansion (5), the auxiliary functions $N_{\alpha_1\alpha_2}(y,\omega^s)$, $C_{\alpha_1}(y,\omega^s)$ and $M(y,\omega^s)$ can be defined by the constructing way analogous to $N_{\alpha_1}(y,\omega^s)$, namely

$$
\begin{cases}
\dfrac{\partial}{\partial y_i}\left(k_{ij}(y,\omega^s)\dfrac{\partial N_{\alpha_1\alpha_2}(y,\omega^s)}{\partial y_j}\right)=\bar{k}_{\alpha_1\alpha_2}(x)-\dfrac{\partial}{\partial y_i}\left(k_{i\alpha_2}(y,\omega^s)N_{\alpha_1}(y,\omega^s)\right)\\
-k_{\alpha_1\alpha_2}(y,\omega^s)-k_{\alpha_2 j}(y,\omega^s)\dfrac{\partial N_{\alpha_1}(y,\omega^s)}{\partial y_j}, \qquad \text{in} \quad Y^{*s}\\
-\nu_i\left(k_{ij}(y,\omega^s)\dfrac{\partial N_{\alpha_1\alpha_2}(y,\omega^s)}{\partial y_j}+k_{i\alpha_2}(y,\omega^s)N_{\alpha_1}(y,\omega^s)\right)=0,\ y\in\Gamma\\
N_{\alpha_1\alpha_2}(y,\omega^s)=0, \qquad y\in\partial Y^s
\end{cases}
\tag{15}
$$

$$
\begin{cases}
\dfrac{\partial}{\partial y_i}\left(k_{ij}(y,\omega^s)\dfrac{\partial C_{\alpha_1}(y,\omega^s)}{\partial y_j}\right)=0, \qquad \text{in } Y^{*s}\\
-\nu_i\left(k_{ij}(y,\omega^s)\dfrac{\partial C_{\alpha_1}(y,\omega^s)}{\partial y_j}\right)\\
=4\sigma\left(N_{\alpha_1}(y,\omega^s)-\int_{\Gamma^c}N_{\alpha_1}(l,\omega^s)F(y,l)dl\right),\ y\in\Gamma\\
C_{\alpha_1}(y,\omega^s)=0, \qquad y\in\partial Y^s
\end{cases}
\tag{16}
$$

$$\begin{cases} \dfrac{\partial}{\partial y_i}\left(k_{ij}(y,\omega^s)\dfrac{\partial M(y,\omega^s)}{\partial y_j}\right) = \rho(y,\omega^s)c(y,\omega^s) - \bar{S}(x), \quad \text{in } Y^{*s} \\ -\nu_i\left(k_{ij}(y,\omega^s)\dfrac{\partial M(y,\omega^s)}{\partial y_j}\right) = 0, \qquad y \in \Gamma \\ M(y,\omega^s) = 0, \qquad\qquad\qquad y \in \partial Y^s \end{cases} \tag{17}$$

where $l = z/\varepsilon$, z is the macroscopic coordinate of the structure, and l is the local coordinate of 1-normalized cell.

Remark 3.1 In order to ensure that $T_\varepsilon(x,\omega,t)$ expressed by (2) satisfy the boundary condition on Γ_1 and Γ_2 in the original problem (1), it is necessary to impose the boundary condition $N_{\alpha_1}(y,\omega^s) = 0$ on ∂Y^s since $\partial T_0(x,t)/\partial x_{\alpha_1}$ do not generally equal to zero on the boundary. Besides, since the distribution of pores in all cells is random, the pore distributions in two adjacent cells are different. Therefore, the configuration of the cells cannot be extended periodically, and the periodicity conditions cannot be used here to construct cell problems (10) and (15)-(17). In order to ensure the existence, uniqueness and whole continuity of solutions, zero-boundary conditions are imposed on the cell problems (10) and (15)-(17).

Remark 3.2 In terms of Lax-Milgram theorem and Poincare's inequality, it is easy to prove that above problems (10) and (15)-(17) have unique solution for any fixed ω^s.

Now, we can define the multiscale approximate solutions of the problem (1) as follows

$$\begin{aligned} T_1^\varepsilon(x,\omega,t) &= T_0(x,t) + \varepsilon N_{\alpha_1}(y,\omega^s)\frac{\partial T_0(x,t)}{\partial x_{\alpha_1}} \\ T_2^\varepsilon(x,\omega,t) &= T_0(x,t) + \varepsilon N_{\alpha_1}(y,\omega^s)\frac{\partial T_0(x,t)}{\partial x_{\alpha_1}} \\ &+\varepsilon^2\left(N_{\alpha_1\alpha_2}(y,\omega^s)\frac{\partial^2 T_0^3(x,t)}{\partial x_{\alpha_1}\partial x_{\alpha_2}} + C_{\alpha_1}(y,\omega^s)T_0^3(x,t)\frac{\partial T_0(x,t)}{\partial x_{\alpha_1}} + M(y,\omega^s)\frac{\partial T_0(x,t)}{\partial t}\right) \end{aligned} \tag{18}$$

where $T_1^\varepsilon(x,\omega,t)$ and $T_2^\varepsilon(x,\omega,t)$ represent the first-order and the second-order multiscale approximate solutions, respectively. Let

$$L_\varepsilon = \rho^\varepsilon(x,\omega)c^\varepsilon(x,\omega)\frac{\partial}{\partial t} - \frac{\partial}{\partial x_i}\left(k_{ij}^\varepsilon(x,\omega)\frac{\partial}{\partial x_j}\right)$$

For any fixed sample ω^s, to compare $T_1^\varepsilon(x,\omega,t)$ with the original solution $T_\varepsilon(x,\omega,t)$, substituting $T_\varepsilon(x,\omega,t) - T_1^\varepsilon(x,\omega,t)$ into (1), we have

$$L_\varepsilon\left(T_\varepsilon(x,\omega,t)-T_1^\varepsilon(x,\omega,t)\right)=f(x,t)+k_{ij}(y,\omega^\varepsilon)\frac{\partial N_{\alpha_1}(y,\omega^\varepsilon)}{\partial y_j}\frac{\partial^2 T_0(x,t)}{\partial x_i\partial x_{\alpha_1}}$$
$$+\frac{\partial}{\partial y_i}\left(k_{ij}(y,\omega^\varepsilon)N_{\alpha_1}(y,\omega^\varepsilon)\right)\frac{\partial^2 T_0(x,t)}{\partial x_j\partial x_{\alpha_1}}+\rho(y,\omega^\varepsilon)c(y,\omega^\varepsilon)\frac{\partial T_0(x,t)}{\partial t}$$
$$+k_{ij}(y,\omega^\varepsilon)\frac{\partial^2 T_0(x,t)}{\partial x_i\partial x_j}+\varepsilon k_{ij}(y,\omega^\varepsilon)\frac{\partial^2}{\partial x_i\partial x_j}\left(N_{\alpha_1}(y,\omega^\varepsilon)\frac{\partial T_0(x,t)}{\partial x_{\alpha_1}}\right)$$
$$+\varepsilon\rho(y,\omega^\varepsilon)c(y,\omega^\varepsilon)N_{\alpha_1}(y,\omega^s)\frac{\partial^2 T_0(x,t)}{\partial t\partial x_{\alpha_1}}$$

It can found that above residual is of order $O(1)$. However, in the practical engineering computation, ε is a fixed smaller constant rather than tending to zero. So the first-order solution is not accepted by the engineers since it is not accurate enough to capture the micro-scale fluctuations inside materials.

In addition, taking $T_\varepsilon(x,\omega,t)-T_2^\varepsilon(x,\omega,t)$ into (1) and considering homogenized Eq. (13), it yields that

$$\begin{aligned}
&L_\varepsilon\left(T_\varepsilon(x,\omega,t)-T_2^\varepsilon(x,\omega,t)\right)=f(x,t)-L_\varepsilon\left(T_2^\varepsilon(x,\omega,t)\right)\\
&=\varepsilon^{-1}\left(\frac{\partial}{\partial y_i}\left(k_{ij}(y,\omega^s)\frac{\partial N_{\alpha_1}(y,\omega^s)}{\partial y_j}\right)+\frac{\partial k_{i\alpha_1}(y,\omega^s)}{\partial y_i}\right)\frac{\partial T_0(x,t)}{\partial x_{\alpha_1}}\\
&+\left[\frac{\partial}{\partial y_i}\left(k_{ij}(y,\omega^s)\frac{\partial N_{\alpha_1\alpha_2}(y,\omega^s)}{\partial y_j}\right)+\frac{\partial}{\partial y_i}\left(k_{i\alpha_2}(y,\omega^s)N_{\alpha_1}(y,\omega^s)\right)\right.\\
&\left.+k_{\alpha_1\alpha_2}(y,\omega^s)+k_{\alpha_2 j}(y,\omega^s)\frac{\partial N_{\alpha_1}(y,\omega^s)}{\partial y_j}-\bar{k}_{\alpha_1\alpha_2}\right]\frac{\partial^2 T_0^3(x,t)}{\partial x_{\alpha_1}\partial x_{\alpha_2}}\\
&+\left[\bar{S}(x)-\rho(y,\omega^\varepsilon)c(y,\omega^\varepsilon)+\frac{\partial}{\partial y_i}\left(k_{ij}(y,\omega^s)\frac{\partial M(y,\omega^s)}{\partial y_j}\right)\right]\frac{\partial T_0(x,t)}{\partial t}\\
&+\frac{\partial}{\partial y_i}\left(k_{ij}(y,\omega^s)\frac{\partial C_{\alpha_1}(y,\omega^s)}{\partial y_j}\right)T_0^3(x,t)\frac{\partial T_0(x,t)}{\partial x_{\alpha_1}}+\varepsilon F_0+\varepsilon^2\frac{\partial}{\partial x_i}F_i
\end{aligned}\tag{19}$$

where

$$
\begin{aligned}
F_0 &= k_{ij}(y,\omega^{\varepsilon})N_{\alpha_1}(y,\omega^{\varepsilon})\frac{\partial^3 T_0}{\partial x_i \partial x_j \partial x_{\alpha_1}} + k_{ij}(y,\omega^{\varepsilon})\frac{\partial N_{\alpha_1\alpha_2}(y,\omega^{\varepsilon})}{\partial y_j}\frac{\partial^3 T_0}{\partial x_i \partial x_{\alpha_1}\partial x_{\alpha_2}} \\
&+ \frac{\partial}{\partial y_i}\left(k_{ij}(y,\omega^{\varepsilon})N_{\alpha_1\alpha_2}(y,\omega^{\varepsilon})\right)\frac{\partial^3 T_0}{\partial x_j \partial x_{\alpha_1}\partial x_{\alpha_2}} + k_{ij}(y,\omega^{\varepsilon})\frac{\partial C_{\alpha_1}(y,\omega^{\varepsilon})}{\partial y_j}\frac{\partial}{\partial x_i}\left(T_0^3\frac{\partial T_0}{\partial x_{\alpha_1}}\right) \\
&+ \frac{\partial}{\partial y_i}\left(k_{ij}(y,\omega^{\varepsilon})C_{\alpha_1}(y,\omega^{\varepsilon})\right)\frac{\partial}{\partial x_j}\left(T_0^3\frac{\partial T_0}{\partial x_{\alpha_1}}\right) + \varepsilon k_{ij}(y,\omega^{\varepsilon})N_{\alpha_1\alpha_2}(y,\omega^{\varepsilon})\frac{\partial^4 T_0}{\partial x_i \partial x_j \partial x_{\alpha_1}\partial x_{\alpha_2}} \qquad (20) \\
&+ \frac{\partial}{\partial y_i}\left(k_{ij}(y,\omega^{s})M(y,\omega^{s})\right)\frac{\partial^2 T_0}{\partial t \partial x_j} + k_{ij}(y,\omega^{s})\frac{\partial M(y,\omega^{s})}{\partial y_j}\frac{\partial^2 T_0}{\partial t \partial x_i} \\
F_i &= k_{ij}(y,\omega^{\varepsilon})C_{\alpha_1}(y,\omega^{\varepsilon})\frac{\partial}{\partial x_j}\left(T_0^3\frac{\partial T_0}{\partial x_{\alpha_1}}\right) + k_{ij}(y,\omega^{s})M(y,\omega^{s})\frac{\partial^3 T_0}{\partial t \partial x_i \partial x_j}
\end{aligned}
$$

By the definitions of $N_{\alpha_1}(y,\omega^s)$, $N_{\alpha_1\alpha_2}(y,\omega^s)$, $C_{\alpha_1}(y,\omega^s)$ and $M(y,\omega^s)$ given by (10) and (15)-(17), the first four terms on the right side of (19) are equal to zero. So the residual of (19) is of order $O(\varepsilon)$. It means that the second-order multiscale solutions are equivalent to the solutions of original problem (1) with order $O(\varepsilon)$ in nearly pointwise sense. This is the reason for seeking second-order two-scale expansions.

Summing up, one obtains following results

Theorem 3.1 The transient conduction and radiation heat transfer problem of random porous materials has statistical multiscale approximate solutions as follows

$$
\begin{aligned}
T_{\varepsilon}(x,\omega,t) &\cong T_0(x,t) + \varepsilon N_{\alpha_1}(y,\omega^s)\frac{\partial T_0(x,t)}{\partial x_{\alpha_1}} \\
&+ \varepsilon^2\left(N_{\alpha_1\alpha_2}(y,\omega^s)\frac{\partial^2 T_0(x,t)}{\partial x_{\alpha_1}\partial x_{\alpha_2}} + C_{\alpha_1}(y,\omega^s)T_0^3(x,t)\frac{\partial T_0(x,t)}{\partial x_{\alpha_1}} + M(y,\omega^s)\frac{\partial T_0(x,t)}{\partial t}\right) \qquad (21)
\end{aligned}
$$

$x \in \Omega^{\varepsilon}$, $y \in Y^{*s}$, $\omega^s \in P$

where $T_0(x,t)$ is the solution of the homogenized problem (13); $N_{\alpha_1}(y,\omega^s)$, $N_{\alpha_1\alpha_2}(y,\omega^s)$, $C_{\alpha_1}(y,\omega^s)$ and $M(y,\omega^s)$ are auxiliary functions defined by (10), and (15)-(17) on the normalized cell Y^{*s}, respectively.

From the formula of temperature (21), the heat flux density is evaluated approximately by

$$
\begin{aligned}
&q_i^{\varepsilon}(x,\omega,t) = -k_{ij}(y,\omega^s)\frac{\partial T_{\varepsilon}(x,\omega^s,t)}{\partial x_j} \\
&= -k_{ij}(y,\omega^s)\frac{\partial T_0(x,t)}{\partial x_j} - k_{ij}(y,\omega^s)\frac{\partial N_{\alpha_1}(y,\omega^s)}{\partial y_j}\frac{\partial T_0(x,t)}{\partial x_{\alpha_1}} \\
&-\varepsilon k_{ij}(y,\omega^s)N_{\alpha_1}(y,\omega^s)\frac{\partial^2 T_0(x,t)}{\partial x_{\alpha_1}\partial x_j} - \varepsilon k_{ij}(y,\omega^s)\frac{\partial N_{\alpha_1\alpha_2}(y,\omega^s)}{\partial y_j}\frac{\partial^2 T_0(x,t)}{\partial x_{\alpha_1}\partial x_{\alpha_2}} \\
&-\varepsilon^2 k_{ij}(y,\omega^s)N_{\alpha_1\alpha_2}(y,\omega^s)\frac{\partial^3 T_0(x,t)}{\partial x_{\alpha_1}\partial x_{\alpha_2}\partial x_j} - \varepsilon k_{ij}(y,\omega^s)\frac{\partial C_{\alpha_1}(y,\omega^s)}{\partial y_j}T_0^3(x,t)\frac{\partial T_0(x,t)}{\partial x_{\alpha_1}} \\
&-\varepsilon^2 k_{ij}(y,\omega^s)C_{\alpha_1}(y,\omega^s)\left(T_0^3(x,t)\frac{\partial^2 T_0(x,t)}{\partial x_{\alpha_1}\partial x_j} + 3T_0^2(x,t)\frac{\partial T_0(x,t)}{\partial x_j}\frac{\partial T_0(x,t)}{\partial x_{\alpha_1}}\right) \\
&-\varepsilon k_{ij}(y,\omega^s)\frac{\partial M(y,\omega^s)}{\partial y_j}\frac{\partial T_0(x,t)}{\partial t} - \varepsilon^2 k_{ij}(y,\omega^s)M(y,\omega^s)\frac{\partial^2 T_0(x,t)}{\partial t\partial x_j}
\end{aligned}
\tag{22}
$$

3.2 Numerical implementation

3.2.1 Finite element (FE) formulations

The computer simulation algorithm developed in Yu et al. [Yu, Cui and Han (2008)] is used to generate a sample with random distribution of pores, and the FE meshes of sample cells applied in this study are those of Han et al. [Han, Cui and Yu (2010)], shown in Fig. 2(a). It can be observed that cell problems (10) and (15)-(17) are all elliptic boundary value problems, and they can be solved by the standard finite element method to get the FE solutions of the first-order and second-order auxiliary functions. And then the homogenized coefficients are evaluated by (11-12) based on the FE solutions of first-order auxiliary functions. Further, the spatial region Ω is divided by using the FE mesh first, shown in Fig. 2(b), and then the temporal domain $(0,t_*)$ is divided by using the backward Euler full discrete format to solve the homogenized problem (13). According to (21) and the FE solutions of auxiliary problems, homogenized coefficients and homogenized problem, the statistical multiscale FE solution of temperature can be evaluated.

3.2.2 Algorithms for statistical multiscale method

The algorithm procedure of statistical multiscale method based on the FE computations for predicting the transient heat conduction-radiation performance is stated as follows

1) Generate a sample ω^s for a unit cell Y^{*s} according to the given probability distribution model P, and determine the material coefficients in (1). Further, partition Y^{*s} into FE meshes.
2) Solve the problem (10) by FE method to get the solution of $N_{\alpha_1}(y,\omega^s)$. Furthermore, the homogenized coefficients $\hat{k}_{ij}(\omega^s)$ and $\hat{S}(\omega^s)$ are calculated through formula (11).

3) Repeat steps 1-2 for L samples $\omega^s (s=1,\cdots,L)$. And the expected homogenized coefficients and cane be evaluated by the formula (12).

4) With the expected homogenized coefficients $\overline{k}_{ij}$ and $\overline{S}$ obtained by step 3, the homogenization solution $T_0(x,t)$ can be obtained through solving problem (13) in $\Omega\times(0,t_*)$ by using FE method and finite difference method.

5) Solve the cell problems (13)-(15) for ω^s by using the same meshes in step 2 to get the FE solutions of $N_{\alpha_1\alpha_2}(y,\omega^s)$, $C_{a_1}(y,\omega^s)$ and $M(y,\omega^s)$.

6) From (21) and (22), the temperature and heat flux density distributions corresponding to the sample ω^s are evaluated.

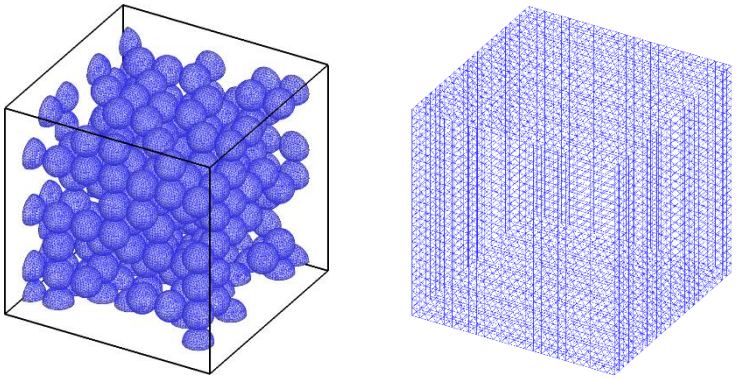

(a) (b)

Figure 2: (a) The meshes of unit cell; (b) the meshes of the homogenized domain Ω

4 Numerical examples

In this section, in order to verify the validity and feasibility of the statistical multiscale analysis method for studying the transient heat conduction problem of random porous materials with nonlinear radiation boundary condition, some numerical examples are given here.

4.1 Validation of the statistical multiscale method

A macrostructure Ω^ε , which is a union of entire periodic cells as shown in Fig. 3(a), is chosen, and the unit cell is depicted in Fig. 3(b). $\overline{T}_1(x)=0K$ and $\overline{T}_2(x)=0K$ are boundary temperatures in x_3-direction. The time step is $\Delta t=0.02$, the radius of the cavity in Y^* is 0.25 and $\sigma=5.669996\times10^{-8}\,W/m^2K^4$.

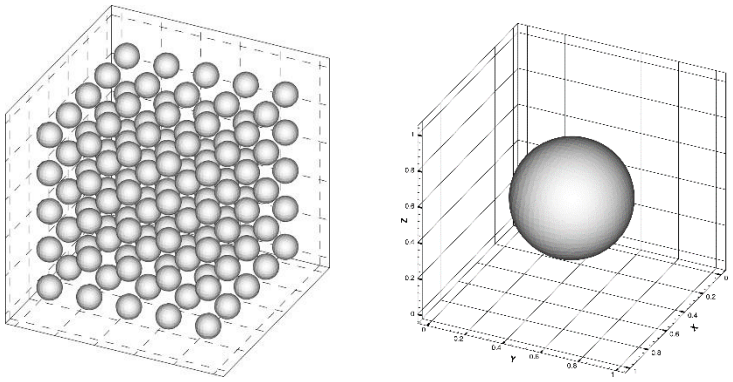

Figure 3: (a) Domain $\Omega^{\varepsilon}=[0,0.25]^3$; (b) Unit cell $Y^*=[0,1]^3$

Since it is difficult to find the analytical solution of above problem, we have to replace $T_{\varepsilon}(x,\omega,t)$ with more precise FE solution T_{FE} in a very fine mesh for comparison. The tetrahedron partition is implemented and the information of the FE meshes is listed in Table 1. Without confusion, it should be noted that $T_0(x,t)$ denotes the numerical solution of the homogenized Eq. (13), $T_1^{\varepsilon}(x,t)$ and $T_2^{\varepsilon}(x,t)$ the first-order and the second-order multiscale numerical solutions based on (21). We consider two cases

Case1： k_{ij} =15 *W/m K*, $f(x)$ =10000 J/m^3s

Case2： k_{ij} =15 *W/m K*, $f(x)$ =100000 J/m^3s

where δ_{ij} is the Kronecker delta.

Table 1: Comparison of computational cost

Elements	Original equation	Unit cell	Homogenized equation
	736815	5817	93750
Nodes	137431	1351	17576

Fig. 4 and Fig. 5 show the numerical results for $T_0(x,t)$, $T_1^{\varepsilon}(x,t)$, $T_2^{\varepsilon}(x,t)$ and T_{FE} at the intersection $x_3=0.15$ and at time $t=0.2$ of different cases. From Fig. 4 and Fig. 5, it can be found that the homogenized solutions, first-order and second-order approximate solutions are in accordance with the FE solutions in the very fine mesh. But Fig. 4 and Fig. 5 demonstrate that the second-order approximate solutions are much better than the homogenized and first-order approximation solutions for temperature. It means that the homogenization solution and the first-order solution are insufficient to describe local fluctuation of the solution. But the second-order multiscale method gives more accurate numerical solutions.

In addition, from Tab. 1, it can be found that the mesh partition numbers of the newly statistical second-order multiscale approximate solution are much less than that of the refined FE solution. It means that the statistical multiscale method can greatly save computer memory and CPU time without losing precision, especially for small ε, which is

very important in actual engineering computation. Both the multiscale and direct FE simulations are performed on the same computer with memory of 512 GB and 16 processors of CPU=2.67 GHz. Actually, it is very cheap by using the statistical multiscale method, taking about 0.8 seconds to finish solving the cell problem and homogenized problem about 6 seconds for one iteration, which takes the majority of the computational efforts. On the other hand, the direct FE simulation takes about 660 seconds because it requires fine meshes.

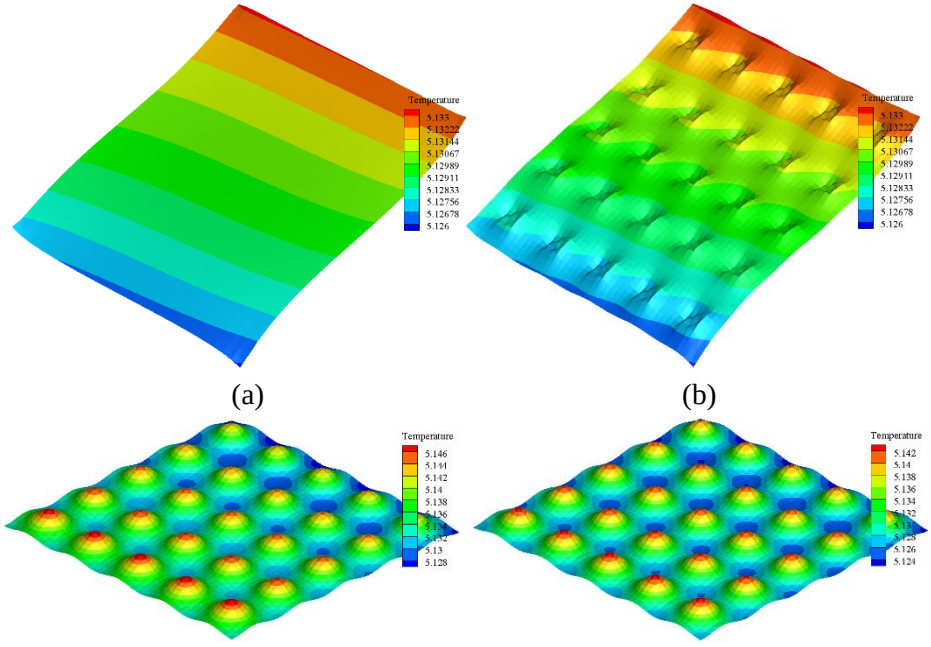

Figure 4: The temperature (*K*) in the cross section x_3=0.15 and at time $t = 0.2$, case 1: (a) $T_0(x,t)$; (b) $T_1^{\varepsilon}(x,t)$; (c) $T_2^{\varepsilon}(x,t)$; (d) T_{FE}

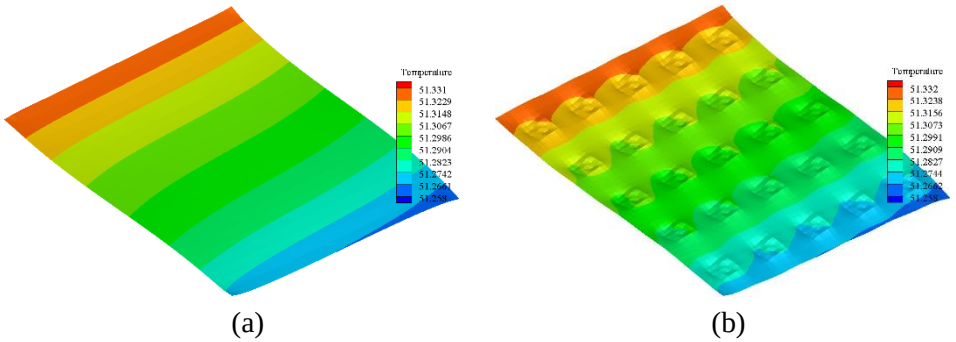

(a) (b)

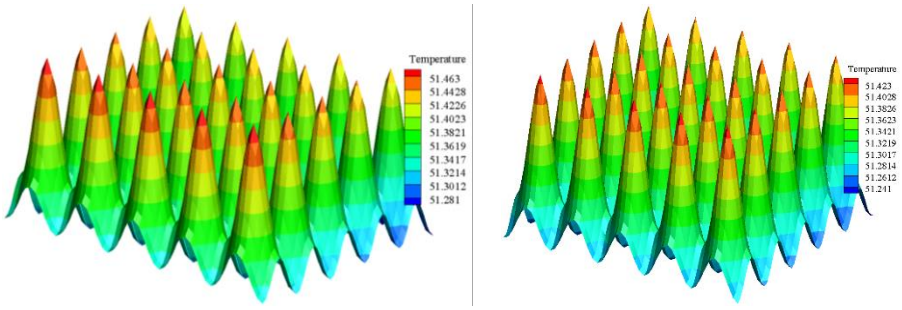

(c) (d)

Figure 5: The temperature (*K*) in the cross section x_3=0.15 and at time $t=0.2$, case 2: (a) $T_0(x,t)$; (b) $T_1^{\varepsilon}(x,t)$; (c) $T_2^{\varepsilon}(x,t)$; (d) T_{FE}

4.2 Influence of micro-structures on the thermal properties and performance

The influence of micro-structures of random porous materials on thermal properties performance is investigated here. Fig. 6 depicts the geometry structure of a plate whose length is 10 mm, width is 10 mm and thickness is 5 mm. The internal heat source $f(x,t)$ is taken as zero, the temperatures in x_3-direction are set as $\bar{T}_1(x,t)$=100K and $\bar{T}_2(x,t)$=1000K on Γ_1, and the thermal conductivity of ceramics is 21.16 *W/mK*.

Porous material structures with three different random distributions of pores are considered: uniformly stochastic distribution of spherical pores in a cell; normally stochastic distribution of spherical pores around the centric point of a cell; uniformly stochastic distribution of ellipsoidal pores whose long axes is about two times of the middle axes and short axes, and which are subjected to normal distribution along x_1-axis, in a cell. Fig. 7 depicts these three samples corresponding to those, which are generated based on Yu et al. [Yu, Cui and Han (2008)]. The radii are both taken as 0.0375 for the pores subjected to uniform distribution and pores subjected to normal distribution. As for the orientations of spherical pores are normal distribution, the sizes of their long axes are taken as 0.1, middle and short axes are both 0.05. The effect of locations, orientations and shapes of pores on thermal properties and performance of the plate are investigated by using the statistical multiscale method. However, due to the pores random dispersion, different samples with the same probability distribution may lead to different numerical results. Therefore, to obtain more accurate prediction values, a number of samples are required.

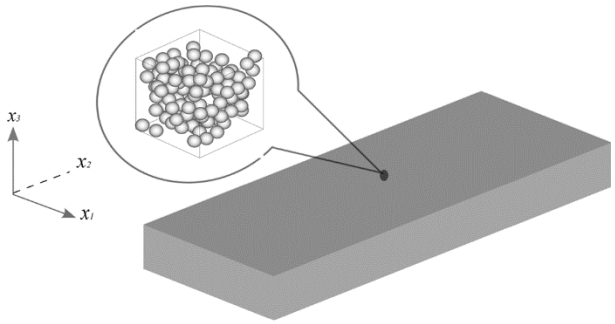

Figure 6: Schematic of porous materials plate

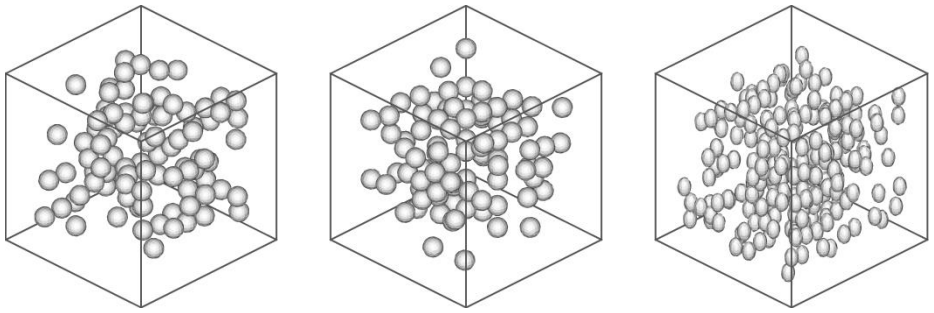

(a) (b) (c)

Figure 7: (a) Uniform distribution; (b) Location-normal distribution; (c) Orientation-normal distribution

Table 2: Orientation-normal distribution with a volume fraction of 20% for different samples

No.	$\bar{k}_{11}$	$\bar{k}_{12}$	$\bar{k}_{13}$	$\bar{k}_{22}$	$\bar{k}_{23}$	$\bar{k}_{33}$
5	16.8624	0.01552	0.008785	16.1757	0.01897	16.1781
10	16.8425	0.00973	0.008701	16.1587	0.01689	16.1399
20	16.8218	0.01631	0.007078	16.1571	0.02285	16.1604
40	16.8317	0.01079	0.015493	16.1506	0.01931	16.1448
50	16.8340	0.01161	0.015572	16.1471	0.01942	16.1505

The expected homogenized thermal conductivity coefficients of porous material with orientation-normal distribution of pores and a volume fraction of 20% for different samples are displayed in Tab. 2. Fig. 8 shows the convergence of expected homogenized parameters with the number of samples. Statistically, different samples should have different numerical results, as shown in Fig. 8. However, as the increasing number of samples with the same random distribution, the mathematical expectation of the computation results

should converge. Obviously, as shown in Fig. 8, the scatter of data decreases with increasing number of samples. As can be seen, 50 samples are chosen in this work to avoid an unacceptable scatter of the computation results.

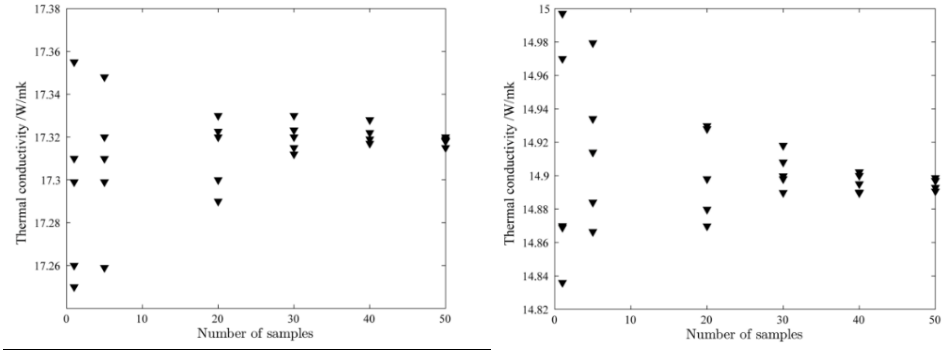

Figure 8: Effective thermal conductivity with different number of samples for two different volume fractions (a) 15%; (b) 25%

Fig. 9 depicts the statistical multiscale results of material parameters and those computed by different analytical methods, i.e. Maxwell-Eucken model [Hashin and Shtrikman (1962)], generalized self-consistent method [Chou, Nomura and Taya (1980)], Cheng-Vachon model [Cheng and Vachon (1969)] and self-consistent method [Hill (1965)]. It can be found that the expected thermal conductivity parameter of porous material with uniform distribution of pores calculated by statistical multiscale method agrees well with the generalized self-consistent method and Maxwell-Eucken model. However, analytical methods cannot obtain satisfactory results for the orientation-normal distribution of spherical pores. Besides, the statistical multiscale results give better approximations than analytical results at lower porosity, as the volume fractions increasing, the deviations of the results increasing. Obviously, it can be concluded that the statistical multiscale method proposed in this paper is sufficiently accurate for predicting the effective properties of the random porous materials. Fig. 10 and Fig. 11 show the local heat flux density distributions in the cells of uniform and orientation-normal distributions with 5.0% and 15.0% of pores at time $t = 1.0$. It can be found that local heat flux densities in different cells have a marked fluctuation. And local heat flux density distributions with a high volume fraction are relatively high. As a result, it can be concluded that the heat flux densities of random porous materials is concurrently affected not only by macroscopic properties, but also by the microscopic structure of random distribution of pores.

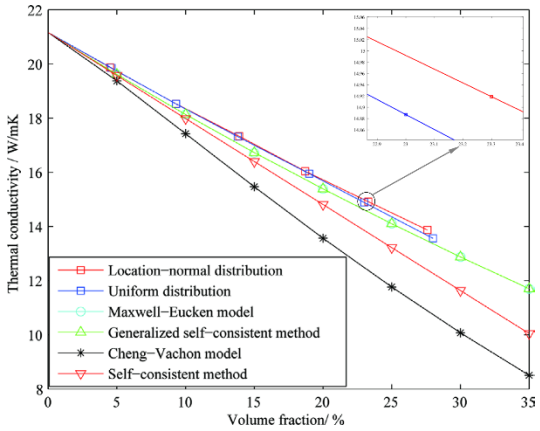

Figure 9: Comparison of the thermal conductivity coefficients obtained from different numerical models: Uniform distribution of pores and location-normal distribution of pores

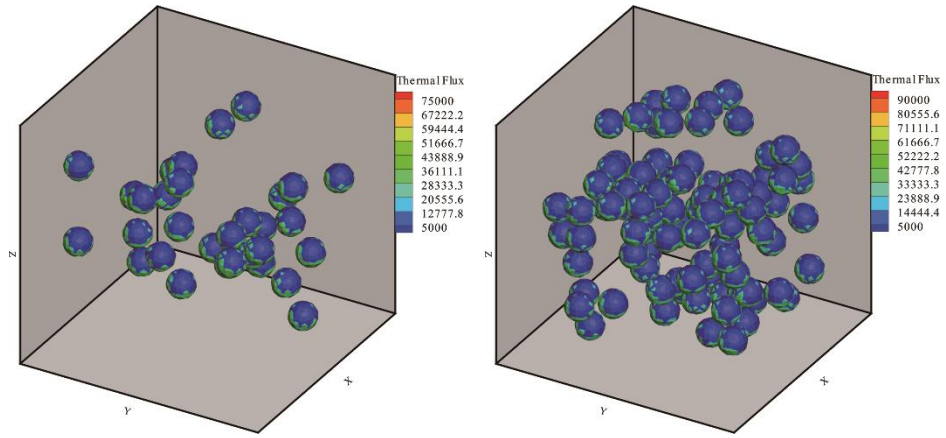

(a) (b)

Figure 10: Heat flux density in local cells with different volume fraction and pores subjected to uniform distribution (a) 5%; (b) 15%

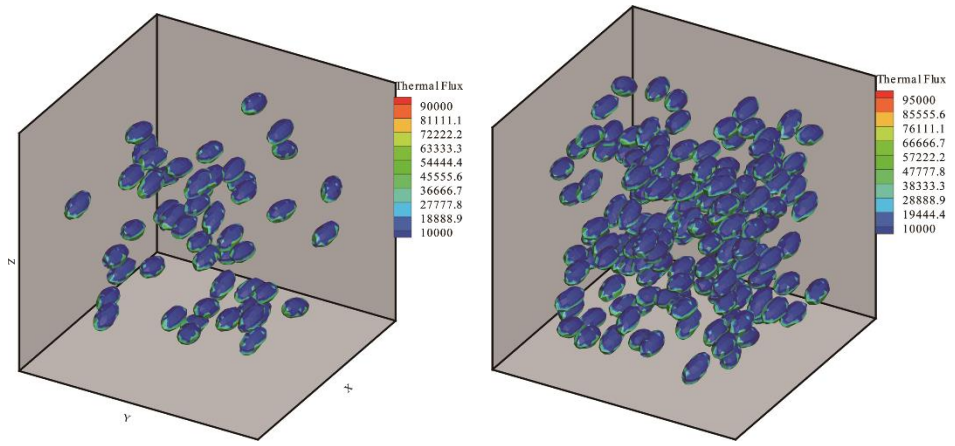

(a) (b)

Figure 11: Heat flux density in local cells with different volume fraction and pores subjected to orientation-normal distribution (a) 5%; (b) 15%

5 Conclusion

This paper presents a statistical multiscale analysis method for a transient heat conduction problem with nonlinear radiation boundary condition in random porous materials. The homogenization and the statistical multiscale formulation are derived in details. A linear homogenized problem independent of radiation effect is obtained, and the second-order correctors featuring nonlinear radiative heat transfer in perforations is introduced, which is absolutely necessary in multiscale simulation of this problem. Error analysis indicates that the second-order multiscale solution has a much better approximation to the solution of the original problem. The validity and effectiveness of the statistical multiscale method and numerical algorithm have been verified by two examples. It was concluded that the statistical multiscale method is accurate to numerically solve the transient conduction and radiation heat transfer problem in random porous materials. Moreover, numerical results also demonstrate that the thermal properties depend greatly on the micro-structures, like volume fraction, location, orientation and spatial distribution of perforations. And local fluctuations of temperature and its gradient can be captured more precisely by adding second-order correctors. As a result, the statistical multiscale analysis method and related numerical approximations techniques proposed can be practically employed to predict the transient heat transfer problem in random porous materials.

Acknowledgement This work was financially supported by the National Natural Science Foundation of China (11501449), the Fundamental Research Funds for the Central Universities (3102017zy043), and the fund of the State Key Laboratory of Solidification Processing in NWPU (SKLSP201628) and the National Key Research and Development Program of China (2016YFB1100602).

References

Allaire, G.; El Ganaoui, K. (2009): Homogenization of a conductive and radiative heat transfer problem. *Multiscale Modeling & Simulation*, vol. 7, pp. 1148-1170.

Amosov, A. A. (2010): Nonstationary radiative-conductive heat transfer problem in a periodic system of grey heat shields. *Journal of Mathematical Sciences*, vol. 169, pp. 1-45.

Bakhvalov, N. S. (1981): Averaging of the heat transfer process in periodic media in the presence of radiation. *Differentsialnye Uravneniya*, vol. 17, pp. 1765-1773.

Bensoussan, A.; Lions, J. L.; Papanicolaou, G. (2011): *Asymptotic analysis for periodic structures*, American Mathematical Society, Rhode Island.

Cheng, S. C.; Vachon, R. I. (1969): The prediction of the thermal conductivity of two and three phase solid heterogeneous mixtures. *International Journal of Heat and Mass Transfer*, vol. 12, pp. 249-264.

Chou, T. W.; Nomura, S.; Taya, M. (1980): A self-consistent approach to the elastic stiffness of short-fibre composites. *Journal of Composite Materials*, vol. 14, pp. 178-188.

Cui, J.; Shih, T. M.; Wang, Y. (1999): The two-scale analysis method for bodies with small periodic configurations. *Structural Engineering and Mechanics*, vol. 7, pp. 601-614.

Efendiev, Y.; Hou, T. Y. (2009): *Multiscale finite element methods: Theory and applications*. Springer Science.

Weinan, E.; Engquist, B.; Li, X.; Ren, W.; Vanden-Eijnden, E. (2007): Heterogeneous multiscale methods: A review. *Computer Physics Communications*, vol. 2, pp. 367-450.

Grujicic, M.; Pandurangan, B.; Zhao, C.; Biggers, S. B.; Morgan, D. R. (2006): Hypervelocity impact resistance of reinforced carbon-carbon/carbon-foam thermal protection systems. *Applied Surface Science*, vol. 252, pp. 5035-5050.

Guan, X.; Liu, X.; Jia, X.; Yuan, Y.; Cui, J. et al. (2015): A stochastic multiscale model for predicting mechanical properties of fiber reinforced concrete. *International Journal of Solids and Structures*, vol. 56, pp. 280-289.

Han, F.; Cui, J.; Yu, Y. (2010): The statistical second-order two-scale method for mechanical properties of statistically inhomogeneous materials. *International Journal for Numerical Methods in Engineering*, vol. 84, pp. 972-988.

Hashin, Z.; Shtrikman, S. (1962): A variational approach to the theory of the effective magnetic permeability of multiphase materials. *Journal of Applied Physics*, vol. 33, pp. 3125-3131.

Hill, R. (1965): A self-consistent mechanics of composite materials. *Journal of the Mechanics and Physics of Solids*, vol. 13, pp. 213-222.

Ishizaki, K.; Komarneni, S.; Nanko, M. (2013): *Porous materials: Process technology and applications*. Springer Science & Business Media.

Jikov, V. V.; Kozlov, S. M.; Oleinik, O. A. (2012): *Homogenization of differential operators and integral functionals*. Springer Science & Business Media.

Juanes, R. (2005): A variational multiscale finite element method for multiphase flow in porous media. *Finite Elements in Analysis and Design*, vol. 41, pp. 763-777.

Li, Y.; Cui, J. (2005): The multi-scale computational method for the mechanics parameters of the materials with random distribution of multi-scale grains. *Composites Science and Technology*, vol. 65, pp. 1447-1458.

Liu, S.; Zhang, Y. (2006): Multi-Scale analysis method for thermal conductivity of porous material with radiation. *Multidiscipline Modeling in Materials and Structures*, vol. 2, pp. 327-344.

Modest, M. F. (2013): *Radiative heat transfer*. Academic Press.

Oleinik, O. A.; Shamaev, A. S.; Yosifian, G. A. (1992): *Mathematical Problems in Elasticity and Homogenization*, North-Holland, Amsterdam.

Park, P. J.; Hou, T. Y. (2004): Multiscale numerical methods for singularly perturbed convection-diffusion equations. *International Journal of Computational Methods*, vol. 1, pp. 17-65.

Sundén, B.; Yuan, J. (2013): Evaluation of models of the effective thermal conductivity of porous materials relevant to fuel cell electrodes. *International Journal of Computational Methods and Experimental Measurements*, vol. 1, pp. 440-455.

Tiihonen, T. (1997): Stefan-Boltzmann radiation on non-convex surfaces. *Mathematical methods in the applied sciences*, vol. 20, pp. 47-57.

Wang, M.; Wang, J.; Pan, N.; Chen, S. (2007): Mesoscopic predictions of the effective thermal conductivity for microscale random porous media. *Physical Review E*, vol. 75, pp. 036702.

Wu, Y.; Xiao, J. (2017): Implementation of the multiscale stochastic finite element method on elliptic PDE problems. *International Journal of Computational Methods*, vol. 14, pp. 1750003.

Yang, Z.; Ma, L.; Ma, Q. (2017): Multiscale nonlinear thermo-mechanical coupling analysis of composite structures with quasi-periodic properties. *Computers, Materials & Continua*, vol. 53, pp. 219-248.

Yang, Z.; Zhang, Y.; Dong, H.; Cui, J. (2017): High-order three-scale method for mechanical behavior analysis of composite structures with multiple periodic configurations. *Composites Science and Technology*, vol. 152, pp. 198-210.

Yang, Z.; Cui, J.; Nie, Y. F.; Ma, Q. (2012): The second-order two-scale method for heat transfer performances of periodic porous materials with interior surface radiation. *Computer Modeling in Engineering & Sciences*, vol. 88, pp. 419-442.

Yu, Y.; Cui, J.; Han, F. (2008): An effective computer generation method for the composites with random distribution of large numbers of heterogeneous grains. *Composites Science and Technology*, vol. 68, pp. 2543-2550.

Zhang, S.; Yang, D.; Zhang, H.; Zheng, Y. (2013): Coupling extended multiscale finite element method for thermoelastic analysis of heterogeneous multiphase materials. *Computers & Structures*, vol. 121, pp. 32-49.